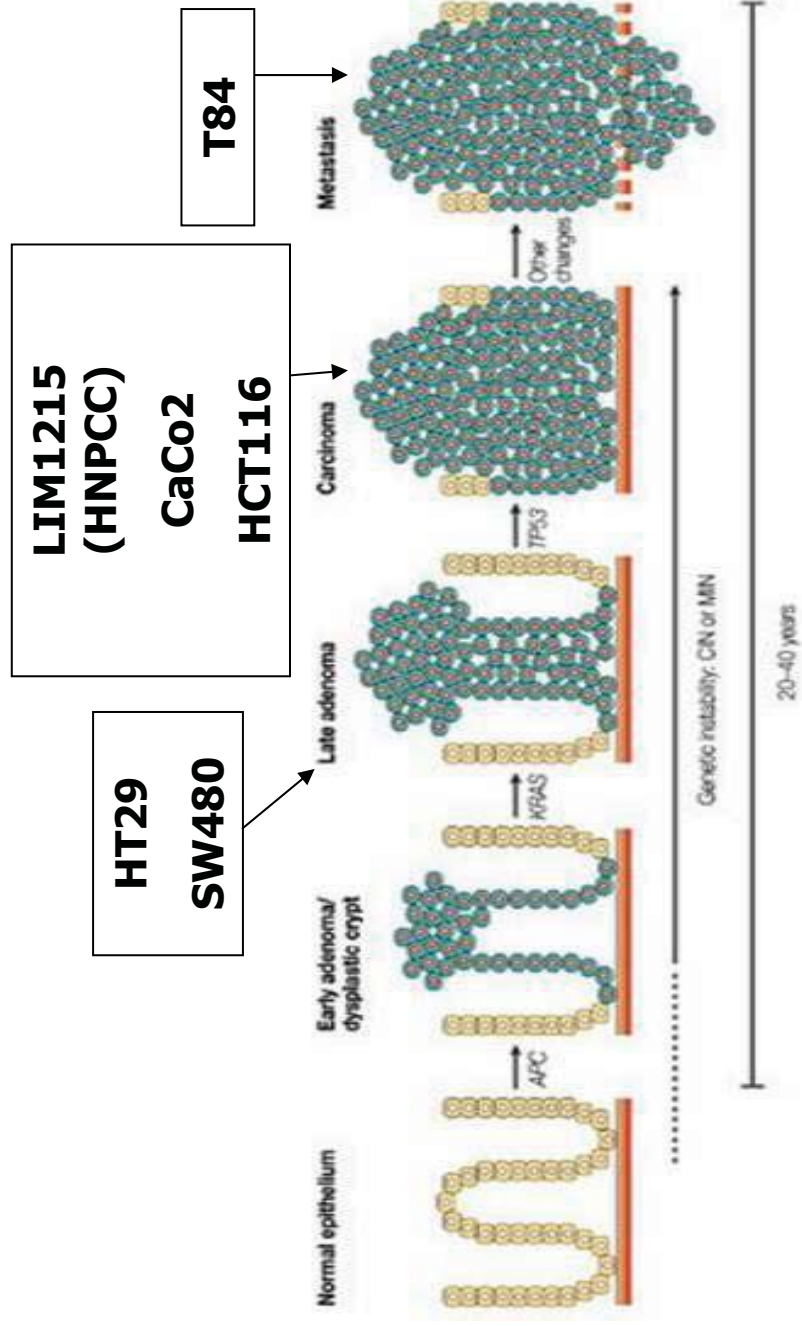


**Figure 1.1: Diagrammatic representation of a colonic crypt.**

The figure illustrates stem cell proliferation, migration, differentiation and apoptosis. The figure was adapted from Chapkin et al 2000.



**Figure 1.2: The relationship between the development and progression of CRC from normal epithelium structure to metastasis.**

This pathway is known as the adenoma to carcinoma pathway. Key gene mutations that occur with the progression of the disease have been identified and named, although other gene mutations may also occur. The position of the 6 different CRC cell lines used in this study along the adenoma to carcinoma pathway are identified. The figure was adapted from Rajagoplan et al 2003.

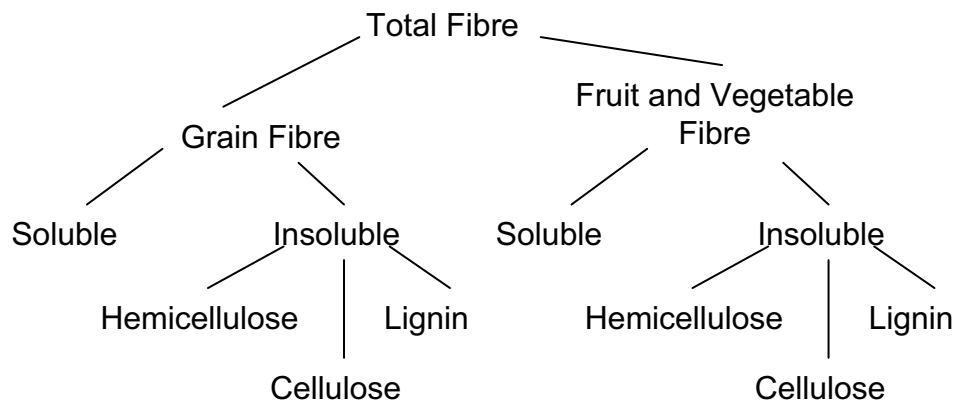


**Figure 1.3: A cascade summarising the components of fibre from different food sources.**

The figure was reproduced from Freudenheim et al 1990.

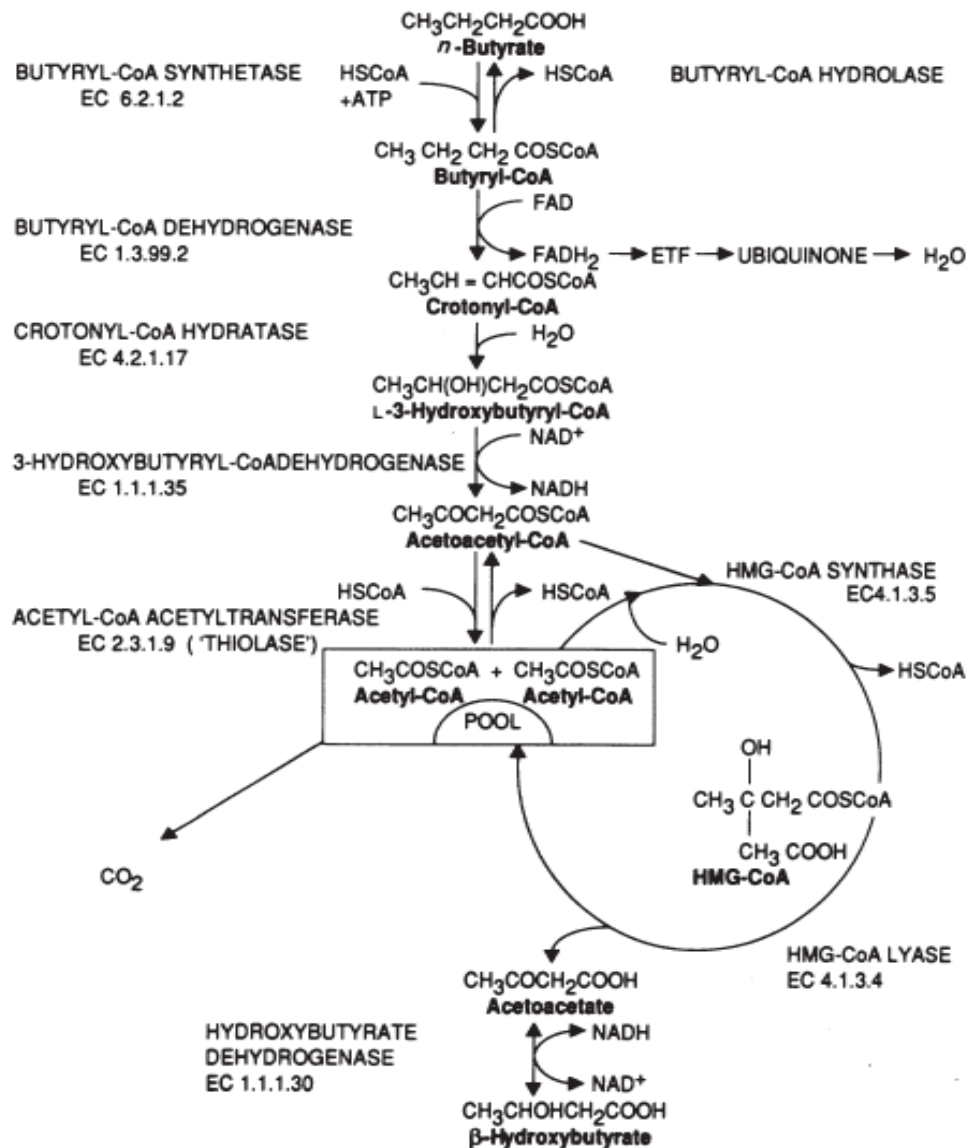


**Figure 1.4: The modulation of BuA by way of the  $\beta$ -oxidation pathway in the HMG-CoA-cycle.**

The figure was reproduced from Wachtershauser et al 2000.

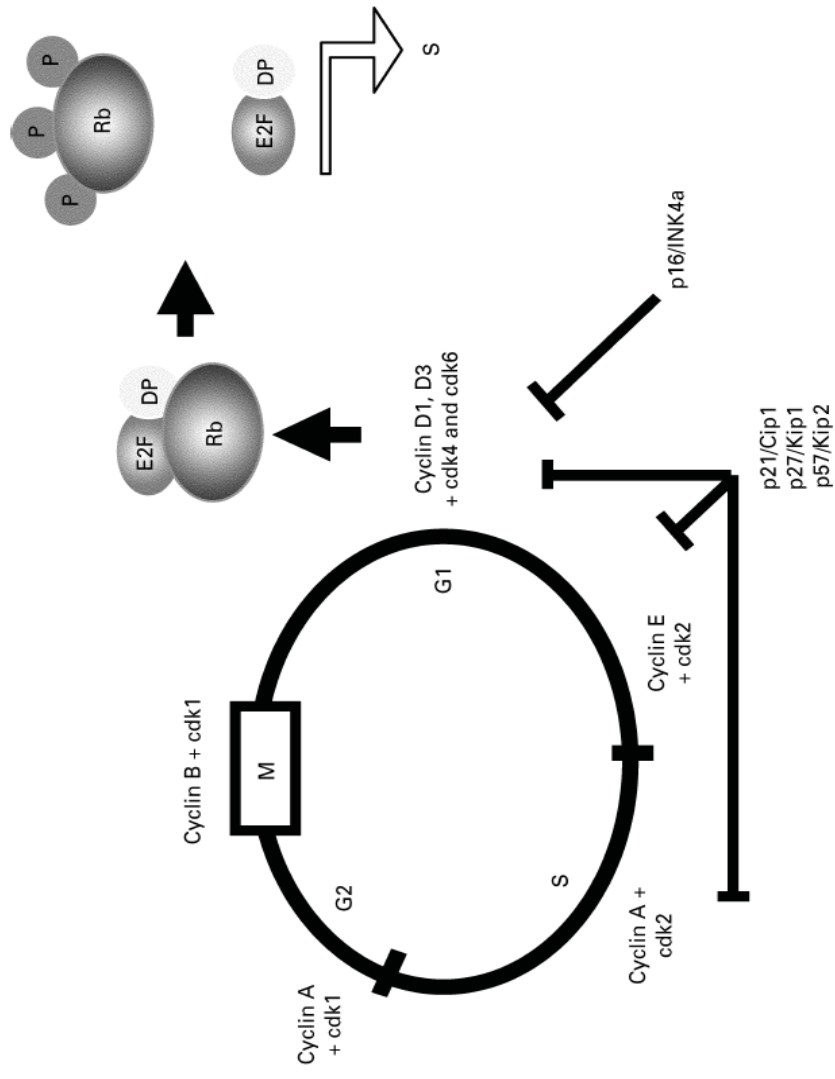


**Figure 1.5: A schematic summary of the key proteins involved in cell cycle regulation and proliferation.**

Note: Cyclins are expressed sequentially during the cell cycle which bind and activate cyclin-dependent kinases (cdk). Inhibitors of the cell cycle belong to 2 families, INK4 and Cip/Kip, which both act to control the activity of cdk. In early G1 phase of the cell cycle, the binding of cyclin D with cdk4 and 6 causes phosphorylation (P) of the retinoblastoma (Rb) protein which enables the release and activation of E2F transcription factor. The figure was reproduced from Blottiere et al 2003.

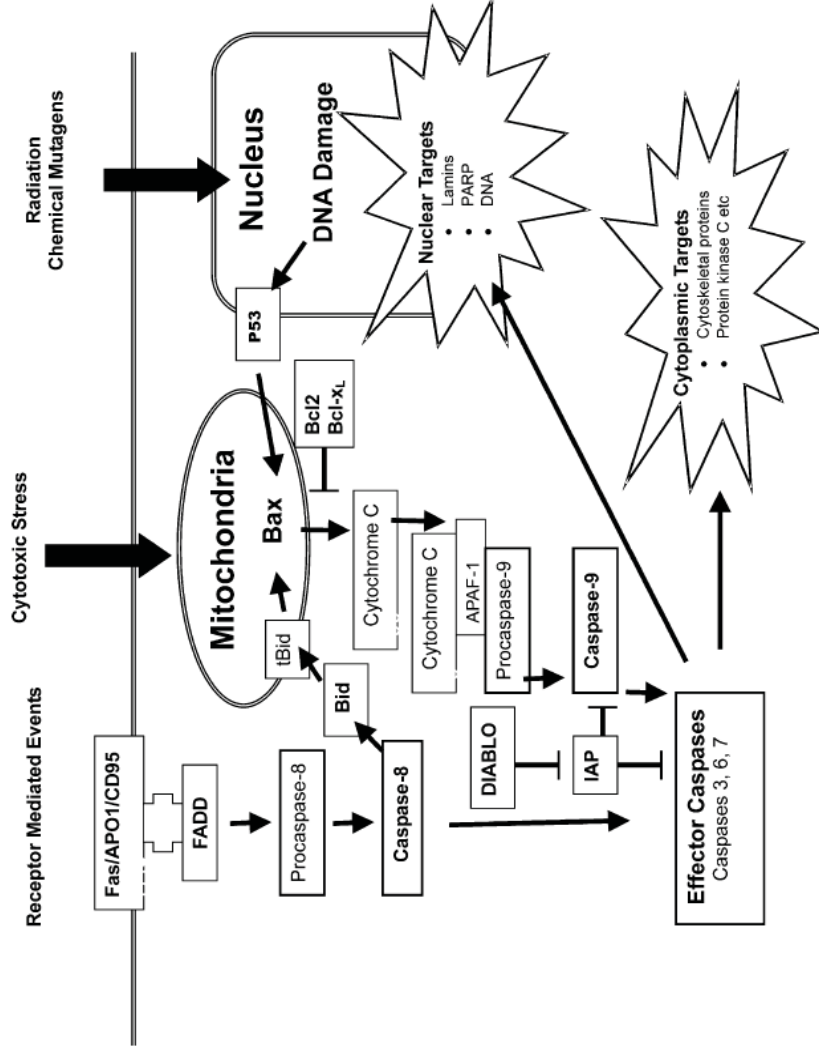


**Figure 1.6: A simplified diagrammatic overview of the initiation and regulation of apoptosis.**

The two main pathways which initiate apoptosis are mediated by cell surface receptors and the mitochondria. Activation of either pathway induces a cascade of secondary events ultimately leading to the activation of effector caspases 3, 6 and 7. Inhibitors of this pathway regulate apoptosis and include the Bcl2, IAP and Bcl-XL proteins. This figure was reproduced from Johnson et al 2002.

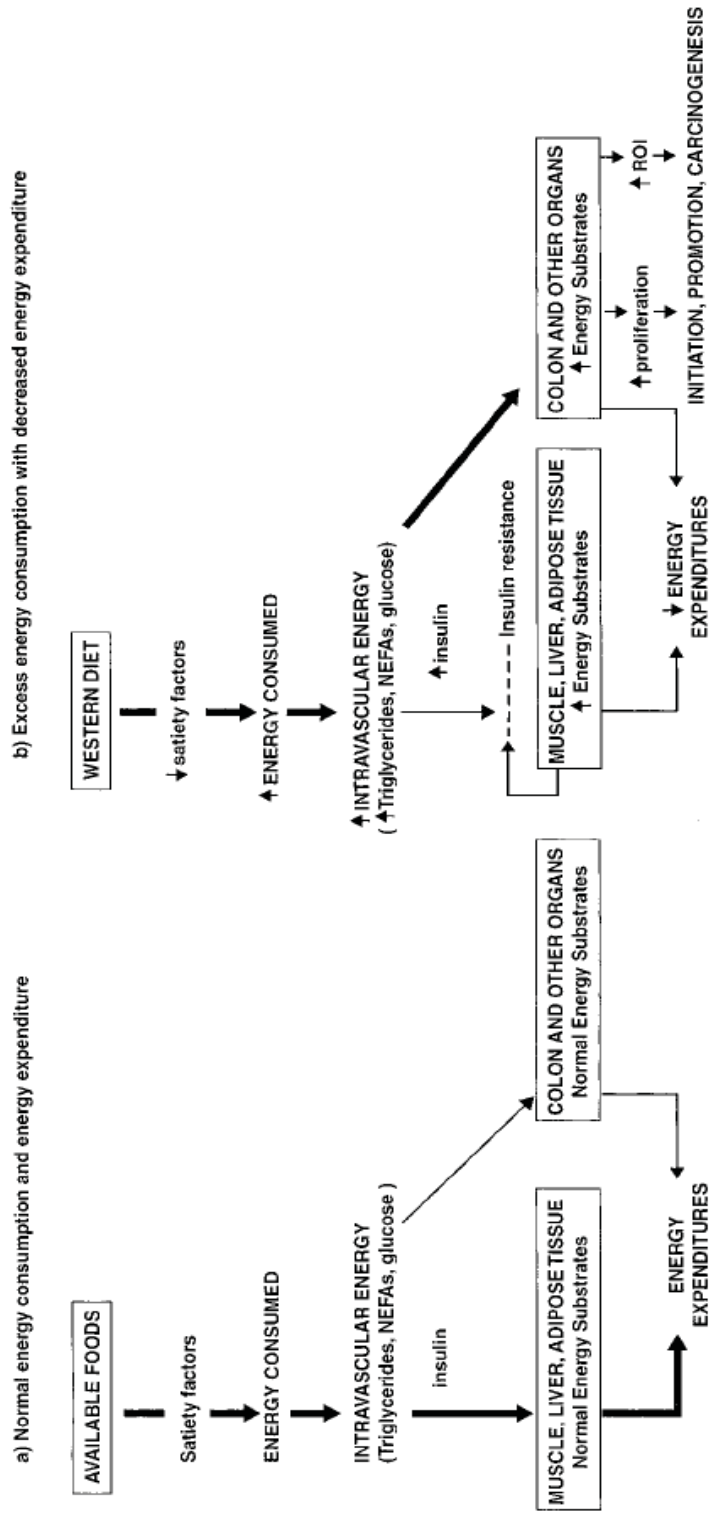


**Figure 1.7: Schematic comparison of the influence of normal and excess energy consumption on the availability of energy to tissues and organs.**

This figure illustrates how the chronic consumption of high energy foods may lead to increased energy availability in the colon; in particular glucose, triglycerides and non essential fatty acids (NEFA). This figure was reproduced from Bruce et al 2000.

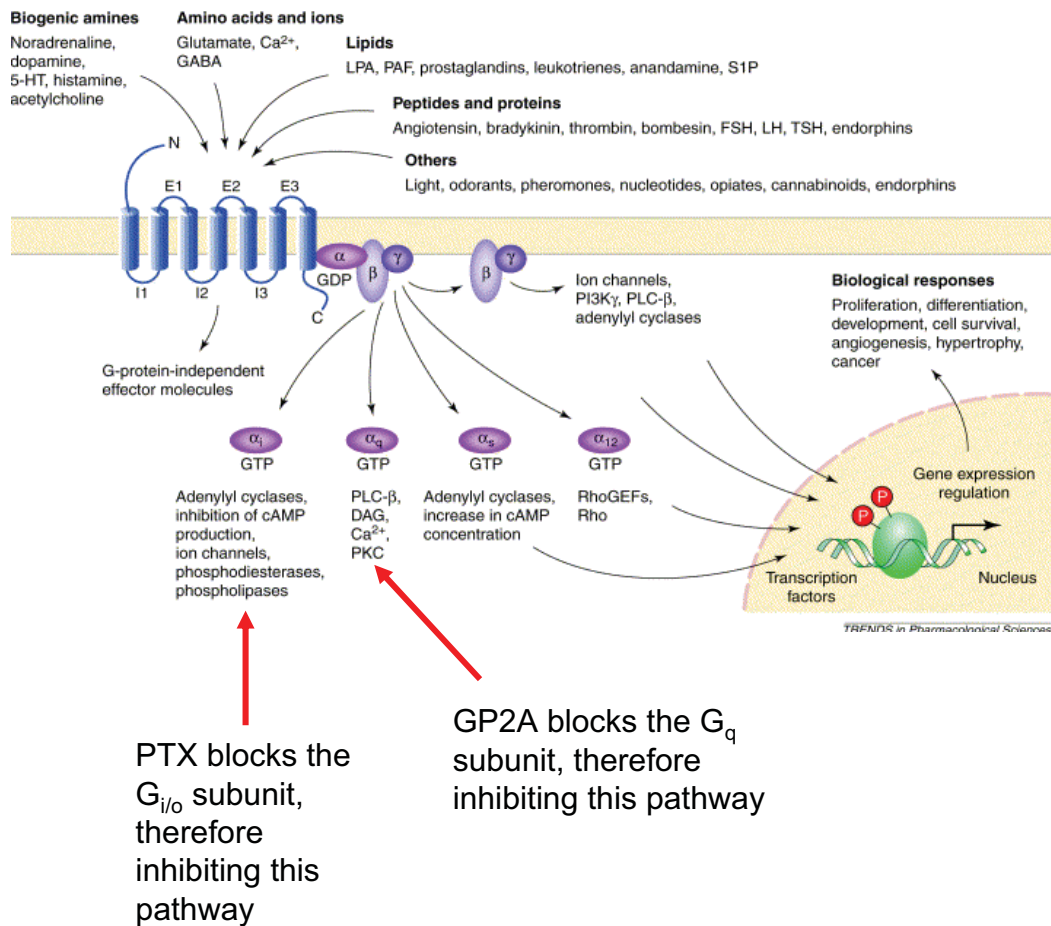


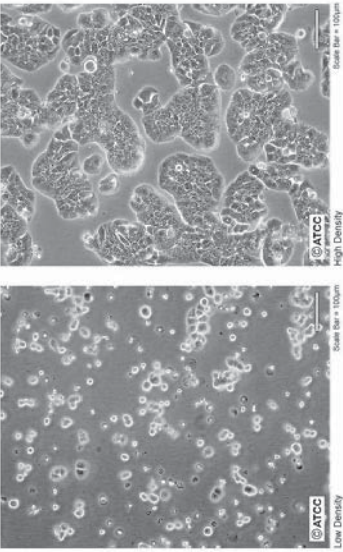
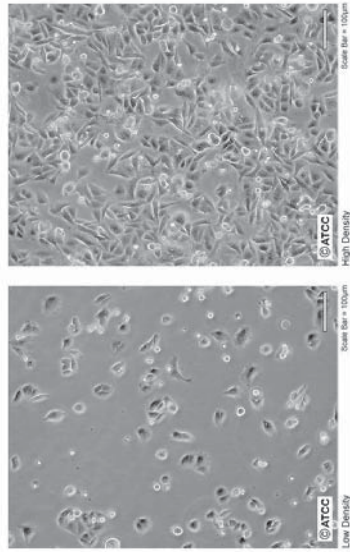
**Figure 1.8: Secondary messenger cascade initiated by agonist induced GPCR activation.**

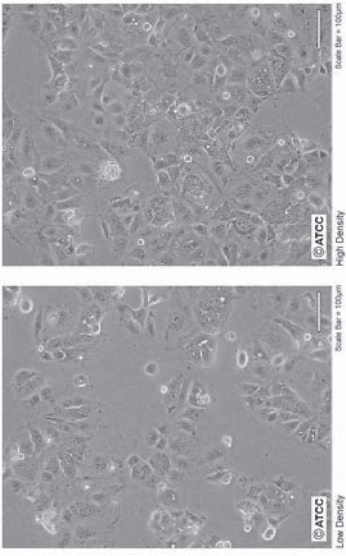
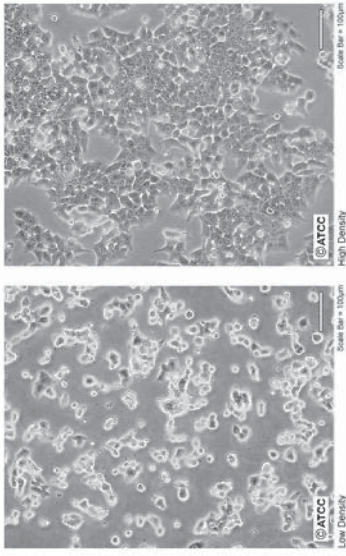
This figure summarises the intricate and highly specialised secondary messenger cascades that are activated by different G<sub>α</sub> subunits, and the different cellular outcomes that arise from activation. Inhibition with G-protein inhibitors PTX and GP2A blocks the activation of the secondary messenger cascades as shown. This figure was adapted from Marinissen and Gutkind 2001.

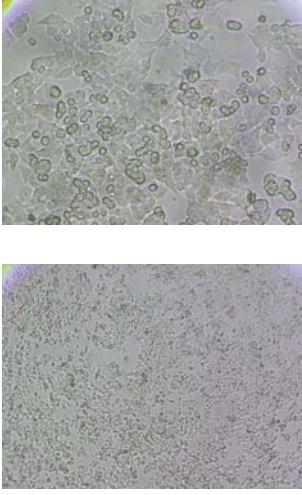
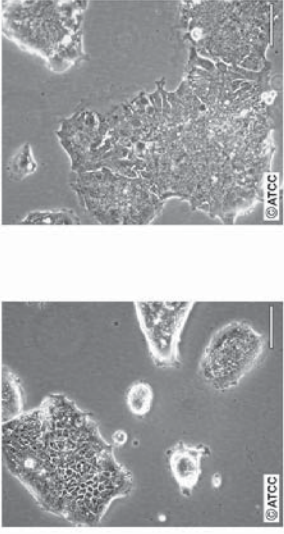


**Table 3.1: The characteristics of 6 CRC cell lines used in this study**

Shown are the photomicrographs of individual CRC cells together with the composition of growth media, the human origin of the cells and the relative growth rate. \* Indicates the split required to produce an 85% confluent flask in 4 days i.e. if split on Monday cells would be confluent Friday.

Cell Line	Morphology	Media composition	Origin	Split*
HT29	<p>Adherent, epithelial</p> <p>ATCC Number: HTB-38 Designation: HT-29</p> 	<p>50% DMEM, 50% HAM (F12), 5% FCS, 1% Pen/Strep</p>	Human colorectal adenocarcinoma	1/10
SW480	<p>Adherent epithelial</p> <p>ATCC Number: CCL-228 Designation: SW 480</p> 	<p>RPMI, 10% FCS, 1% Pen/Strep</p>	Human colorectal adenocarcinoma	1/10

CaCo2	<p>Adherent, small clusters of vacuolar cells and single round cells</p> <p>ATCC Number: <b>HIB-37</b> Designation: <b>Caco-2</b></p> 	<p>DMEM, 20% FCS, 1% 100mM pyruvate, 1% non-essential amino acids 1% Pen/Strep</p>	Human colon carcinoma	1/5
HCT116	<p>Adherent epithelial</p> <p>ATCC Number: <b>CCL-247</b> Designation: <b>HCT 116</b></p> 	<p>McCoy's, 10% FCS and 1% Pen/Strep</p>	Human colon carcinoma	1/12

LIM1251	<p>Adherent but loosely attaching. Round up more as they get confluent</p> 	RPMI, 10% FCS, 1% Pen/Strep	Human colon carcinoma- HPNCC	1/10
T84	<p>Adherent epithelial</p> <p>ATCC Number: <b>CCL-248</b> Designation: <b>T84</b></p> 	50% DMEM, 50% HAM (F12), 10% FCS, 1% Pen/Strep	Human colorectal carcinoma (metastatic site; lung)	1/5

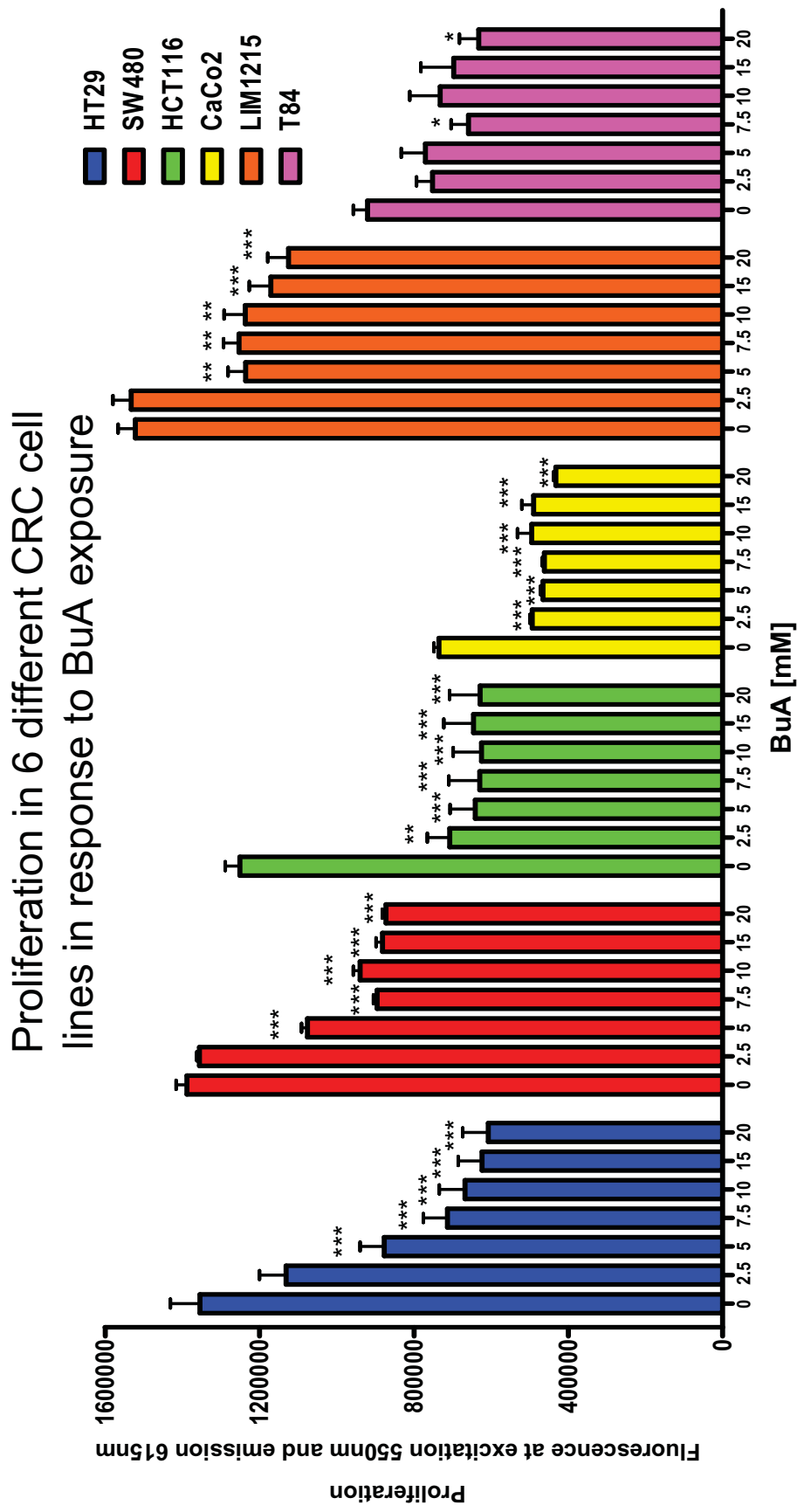


**Figure 3.1: A comparison of the proliferative response of 6 CRC cell lines to varying BuA concentrations for 48 hours.**

Each assay was conducted in triplicate with 3 separate replicates with the means  $\pm$  SEM shown. . Statistical analysis was conducted using One-way ANOVA with Tukey's post-hoc testing. (\*)  $p < 0.05$  (\*\*)  $p < 0.01$  (\*\*\*)  $p < 0.001$  denotes significance compared to 0mM BuA for each cell line.

## Apoptosis in 6 different CRC cell lines

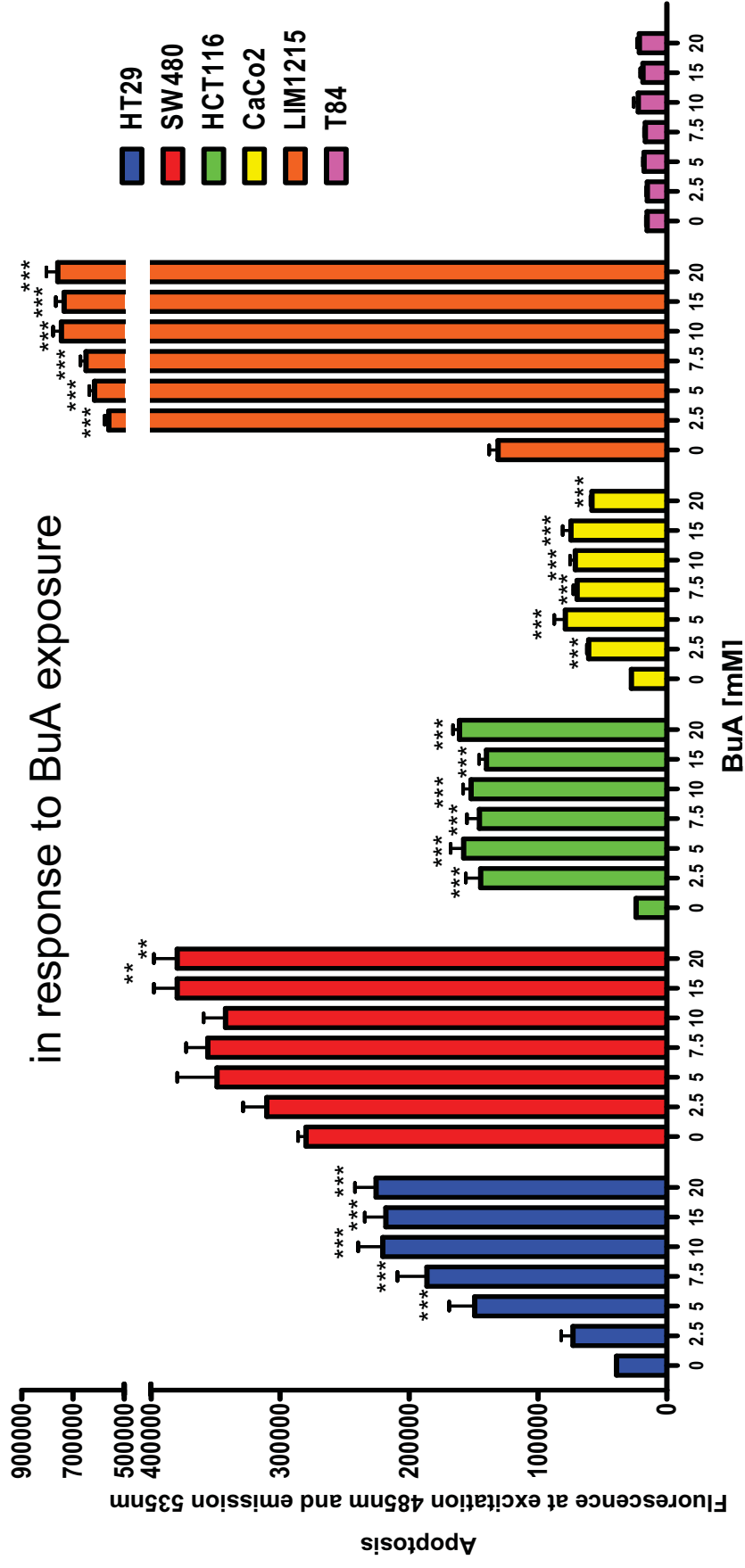
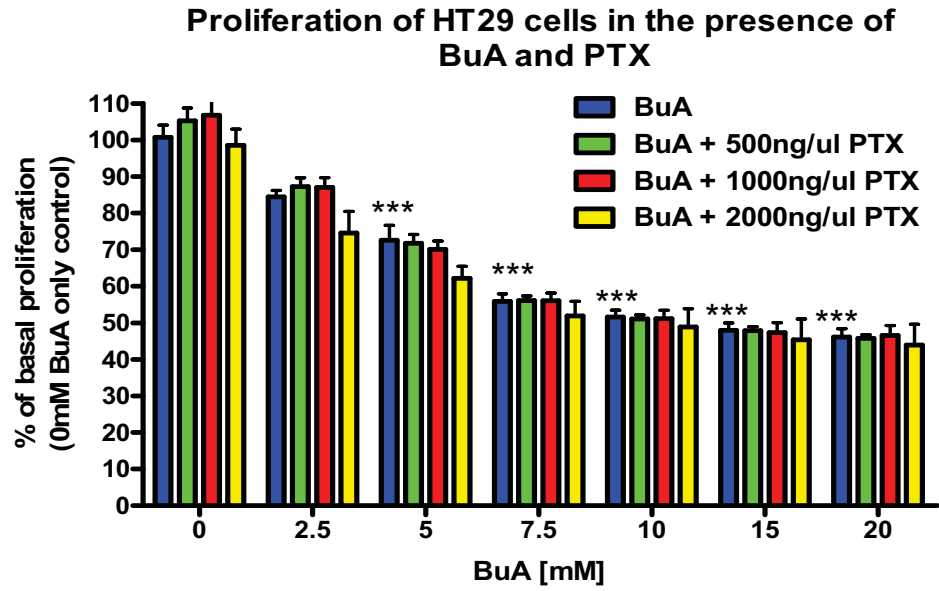


**Figure 3.2: A comparison of the apoptotic response of 6 CRC cell lines to varying BuA concentrations for 48 hours.**

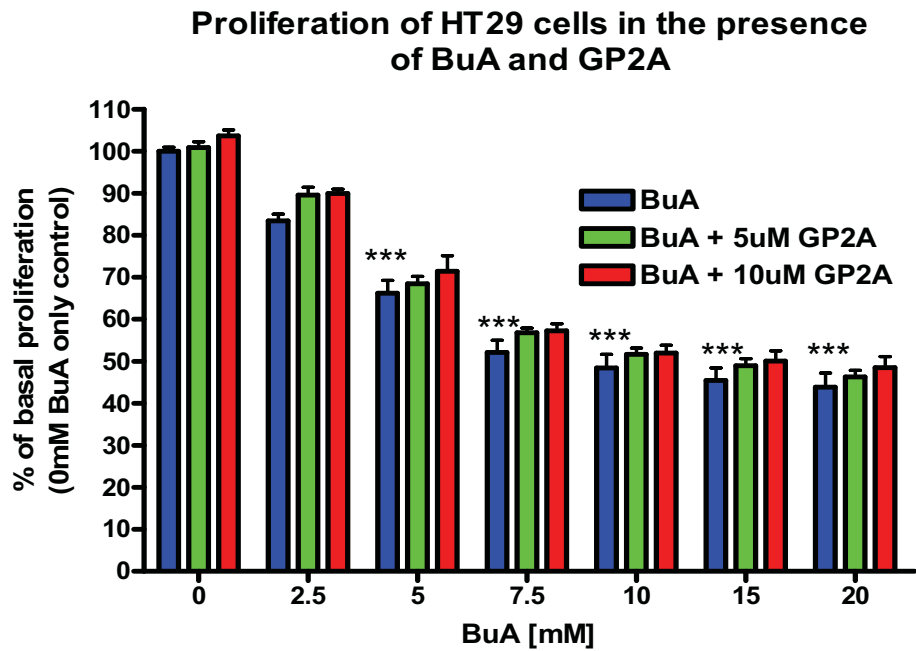
Each assay was conducted in triplicate with 3 separate replicates with the means  $\pm$  SEM shown. Statistical analysis was conducted using One-way ANOVA with Tukey's post-hoc testing. (\*)  $p < 0.05$  (\*\*)  $p < 0.01$  (\*\*\*)  $p < 0.001$  denotes significance compared to 0mM BuA for each cell line.

Figure 3.3

a



b



**Figure 3.3: The influence of G-protein inhibition on the proliferation of untreated and BuA treated HT29 cells.**

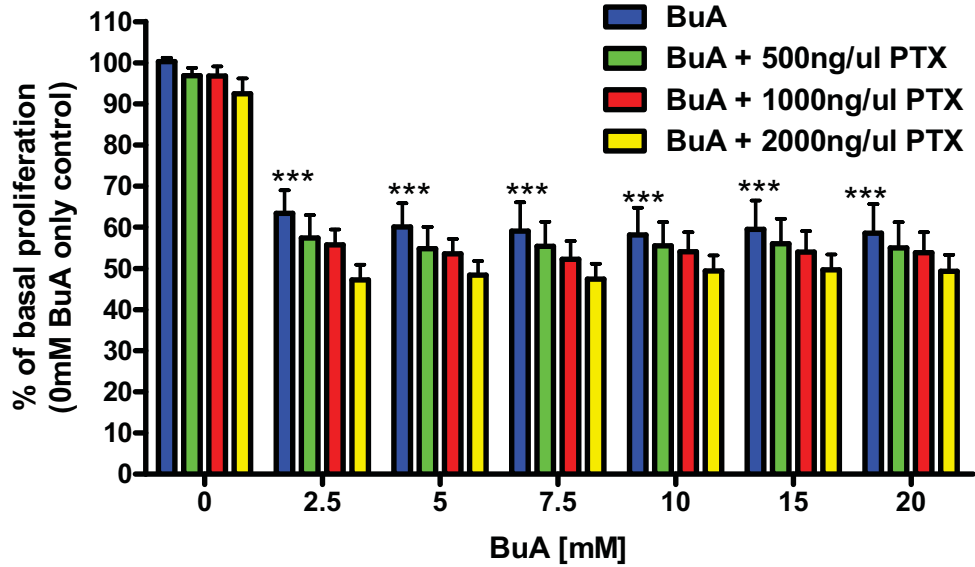
Cells were treated with the G-protein inhibitors PTX (a) and GP2A (b) for 48 hours as described in the text. Each assay was conducted in triplicate with 3 separate replicates with the means  $\pm$  SEM shown. Statistical analysis was conducted using One-way ANOVA with Tukey's post-hoc testing.

(\*)  $p < 0.05$  (\*\*)  $p < 0.01$  (\*\*\*)  $p < 0.001$  denotes significance compared to 0mM BuA alone.

(#)  $p < 0.05$  (##)  $p < 0.01$  (###)  $p < 0.001$  denotes significance compared to BuA alone at each concentration tested.

Figure 3.4

a Proliferation of HCT116 cells in the presence of BuA and PTX



b

Proliferation of HCT116 cells in the presence of BuA and GP2A

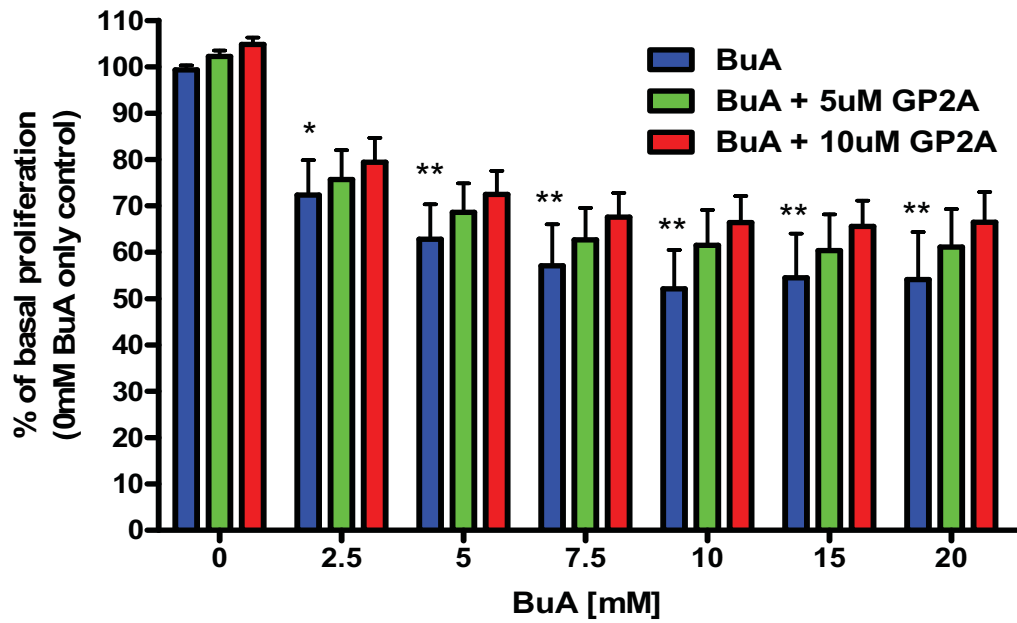




**Figure 3.4: The influence of G-protein inhibition on the proliferation of untreated and BuA treated HCT116 cells.**

Cells were treated with the G-protein inhibitors PTX (a) and GP2A (b) for 48 hours as described in the text. Each assay was conducted in triplicate with 3 separate replicates with the means  $\pm$  SEM shown. Statistical analysis was conducted using One-way ANOVA with Tukey's post-hoc testing.

(\*)  $p < 0.05$  (\*\*)  $p < 0.01$  (\*\*\*)  $p < 0.001$  denotes significance compared to 0mM BuA alone.

Figure 3.5

a

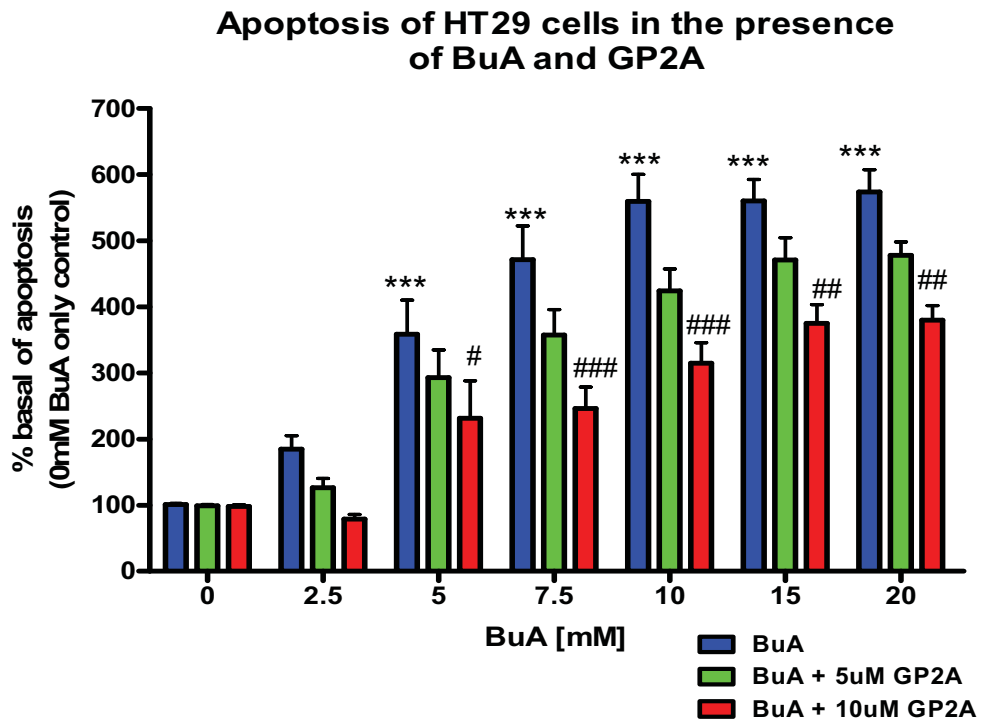
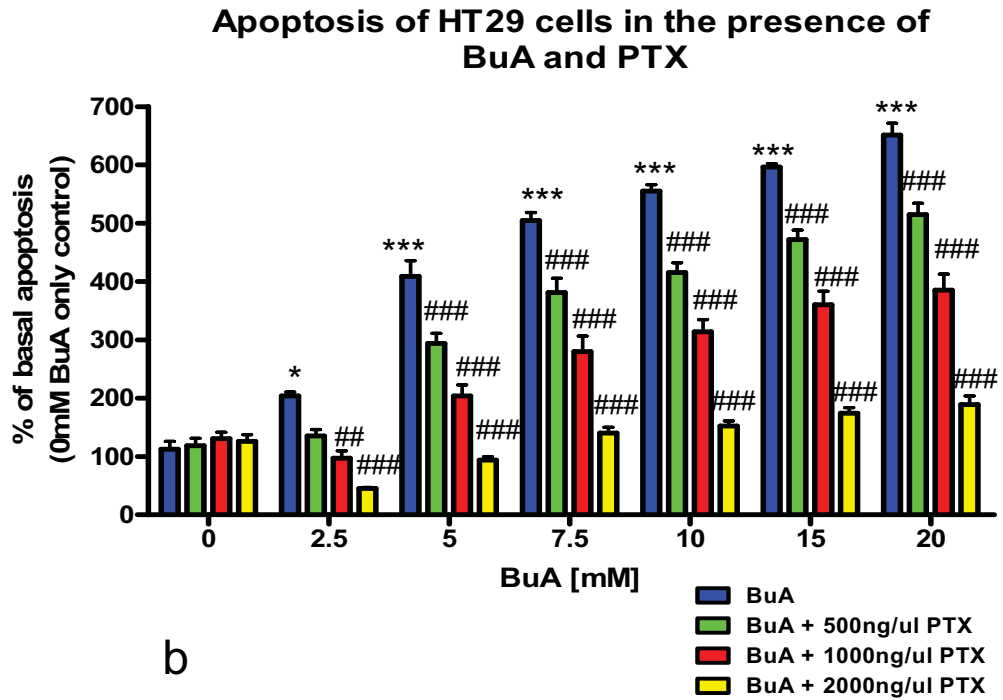


**Figure 3.5: The influence of G-protein inhibition on the apoptosis of untreated and BuA treated HT29 cells.**

Cells were treated with the G-protein inhibitors PTX (a) and GP2A (b) for 48 hours as described in the text. Each assay was conducted in triplicate with 3 separate replicates with the means  $\pm$  SEM shown. Statistical analysis was conducted using One-way ANOVA with Tukey's post-hoc testing.

(\*)  $p < 0.05$  (\*\*)  $p < 0.01$  (\*\*\*)  $p < 0.001$  denotes significance compared to 0mM BuA alone.

(#)  $p < 0.05$  (##)  $p < 0.01$  (###)  $p < 0.001$  denotes significance compared to BuA alone at each concentration tested.

Figure 3.6

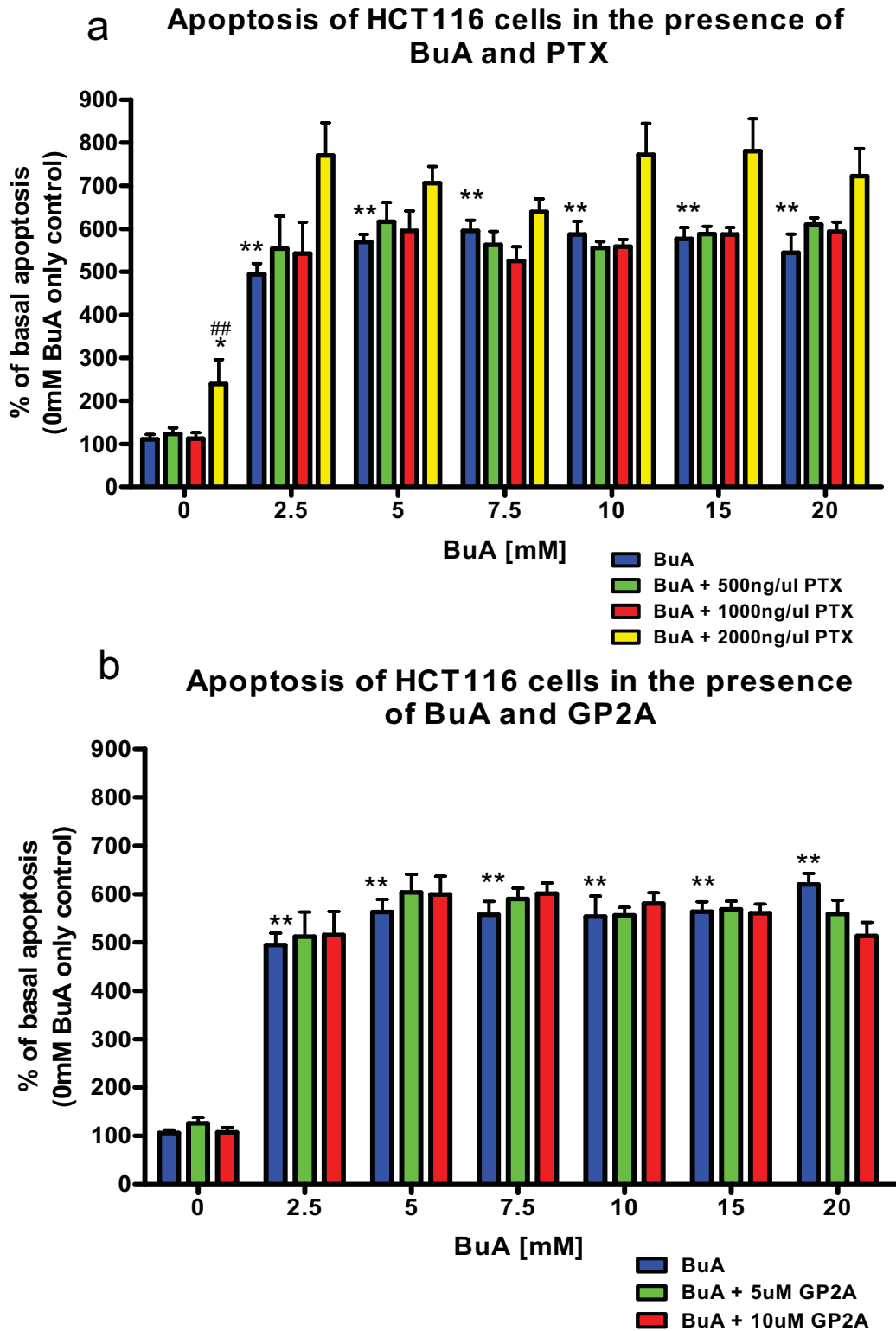


**Figure 3.6: The influence of G-protein inhibition on the apoptosis of untreated and BuA treated HCT116 cells.**

Cells were treated with the G-protein inhibitors PTX (a) and GP2A (b) for 48 hours as described in the text. Each assay was conducted in triplicate with 3 separate replicates with the means  $\pm$  SEM shown. Statistical analysis was conducted using One-way ANOVA with Tukey's post-hoc testing.

(\*)  $p < 0.05$  (\*\*)  $p < 0.01$  (\*\*\*)  $p < 0.001$  denotes significance compared to 0mM BuA alone.

**Figure 4.1: Electrophoretic analysis of RNA extracted from human cell lines and PBMCs.**

RNA was extracted from the U937 monocytic cell line (a), Human PBMC cells (b) and the 6 Human CRC cell lines used in this study (c). The RNA was subjected to electrophoresis and stained as described in the text.

The results show strong bands in all samples at 2.7kb and 1.1kb which are indicative of the 28S and 18S ribosomal RNA, demonstrating the quality and integrity of the RNA from each of the extractions. Shown are the molecular weight markers and the lanes representing RNA from the extracts are indicated. The precise details are described in the text.

Figure 4.1

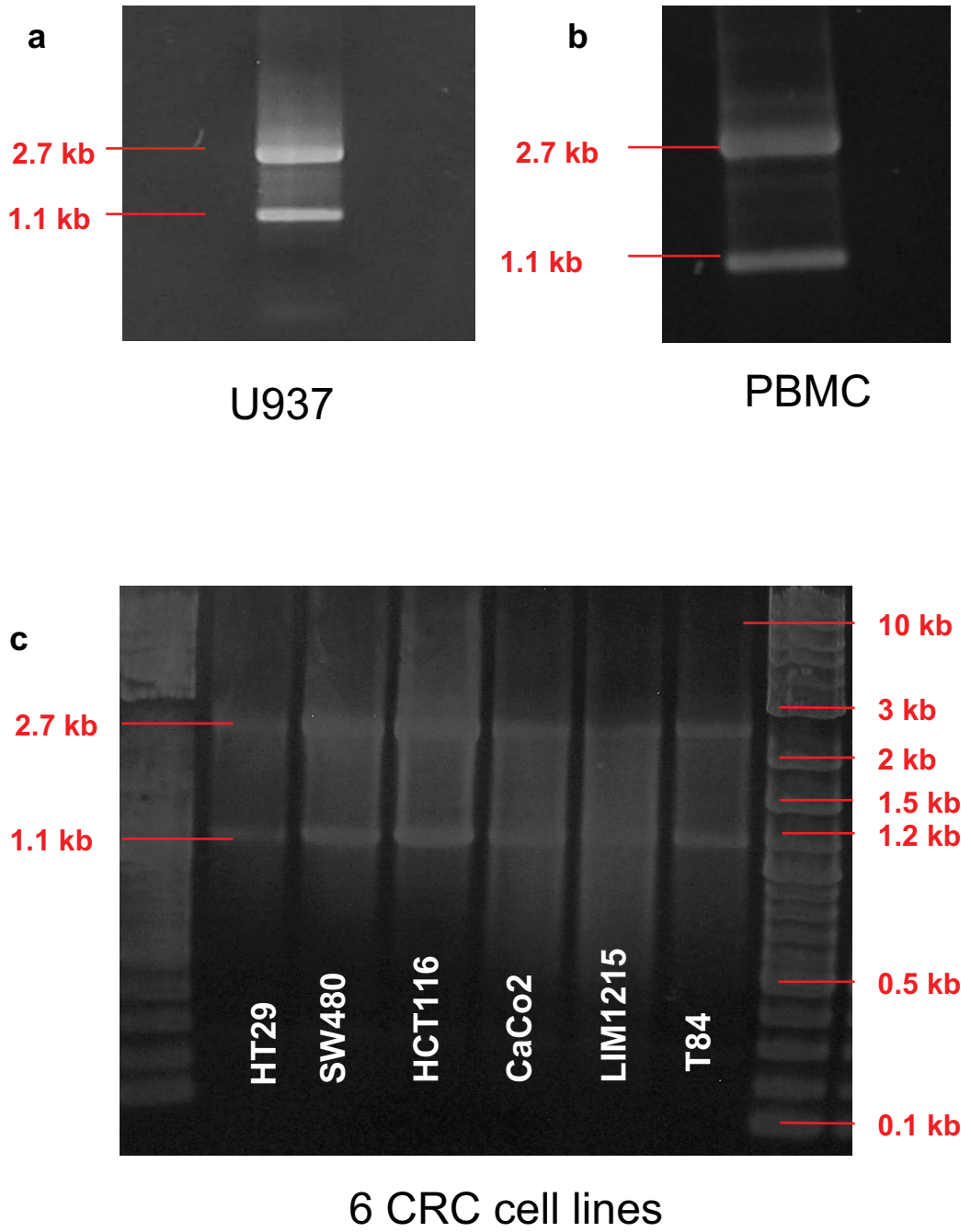


**Figure 4.2: Electrophoretic analysis of RT-PCR amplicons, including controls, from U937 monocytic cell lines and isolated human PBMC cells.**

Amplification products from PCR reactions using PBMC extracts were shown in panel (a) and corresponding products from PBMC in panel (b). In both panels the amplicons shown were:

Lane 1) RNA sample using 330bp GPCR43 primer set.  
Lane 2) cDNA sample using 330bp GPCR43 primer set,  
Lane 3) RNA sample using 993bp GPCR43 primer set,  
Lane 4) cDNA sample used with 993bp GPCR43 primer set,  
Lane 5) cDNA used with housekeeping gene  $\beta$ -actin.

In panel (a) Lane 6) represents the no template control for the  $\beta$ -actin housekeeping gene.

In panel (b) Lane 6) represents the no template control for the 330bp GPCR43 primer set, and Lane 7) no template control for the 993bp GPCR43 primer set.

Also shown are the molecular weight markers. The precise details are described in the text.



Figure 4.2

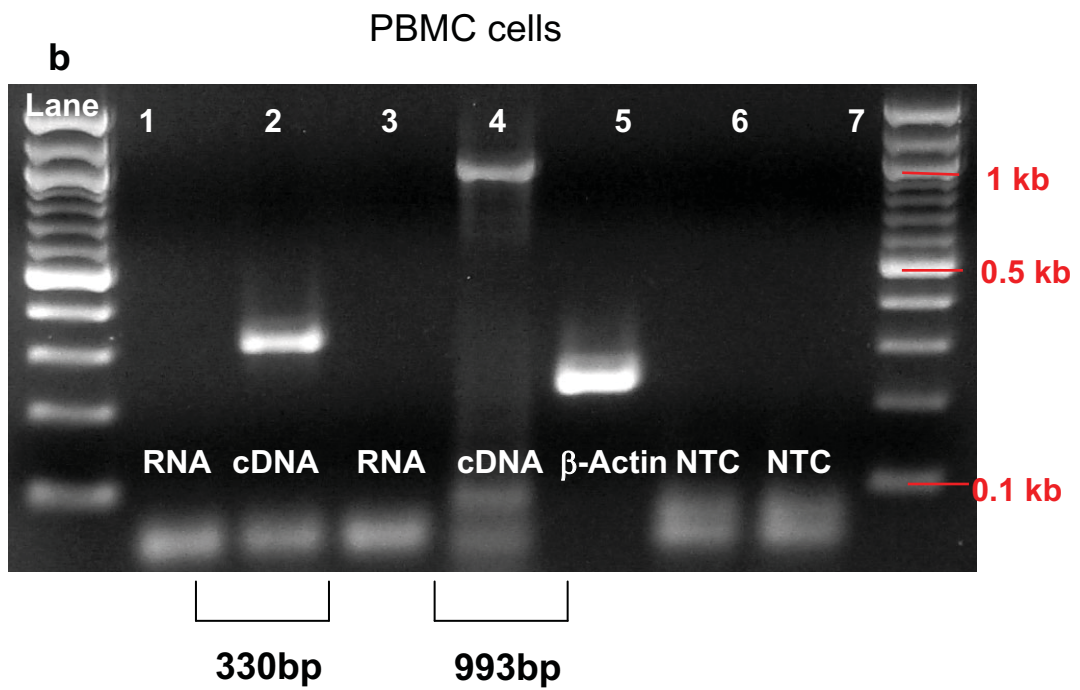
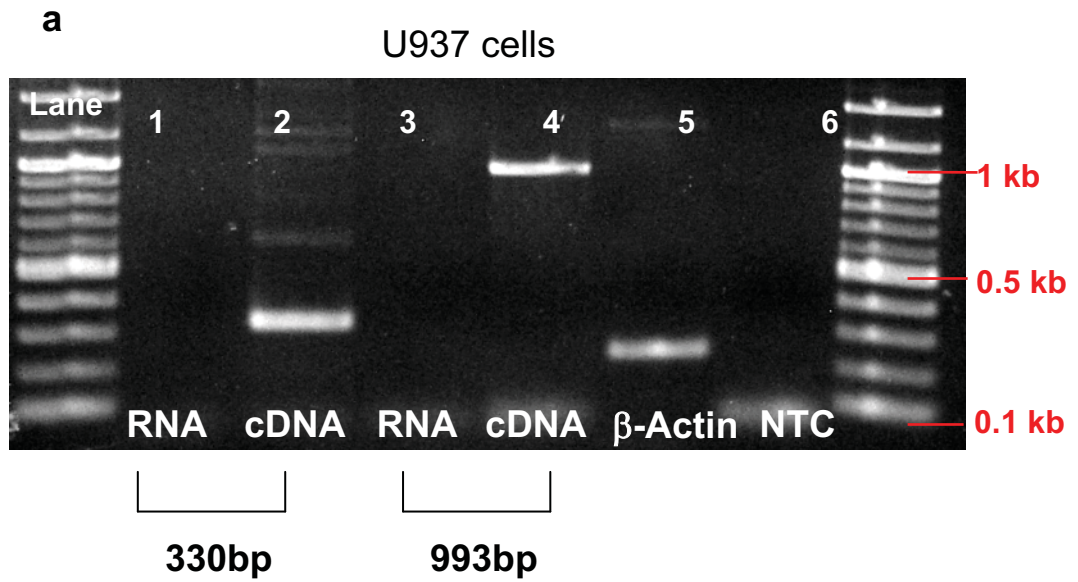
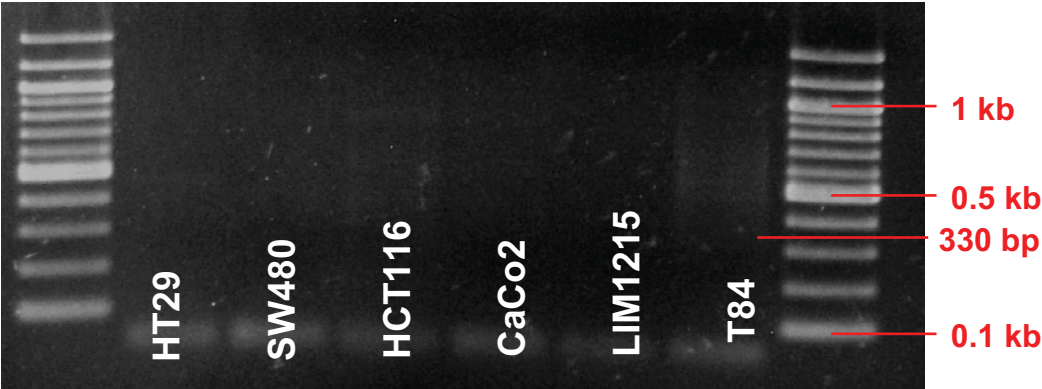


**Figure 4.3: Electrophoretic analysis of RT-PCR amplicons generated from non-transcribed cDNA samples illustrating an absence of gDNA contamination.**

Shown are the electrophoretic analysis of RT-PCR amplicons using primers to amplify 330bp fragments (a) and 993bp fragments (b). The 6 CRC cell lines examined in this study are shown as are the molecular weight markers. The precise details are described in the text.

Figure 4.3

a



b



**Figure 4.4: Electrophoretic analysis indicating  $\beta$ -Actin expression is consistent across 6 CRC cell lines.**

Shown is the consistent expression of  $\beta$ -Actin across each of the 6 CRC cell lines using:

- (a) Gel electrophoresis of RT-PCR amplicons.
- (b) Densitometry of band intensity of  $\beta$ -Actin expression using Scion Image software.

The molecular weight markers are shown with the precise details described in the text.

Figure 4.4

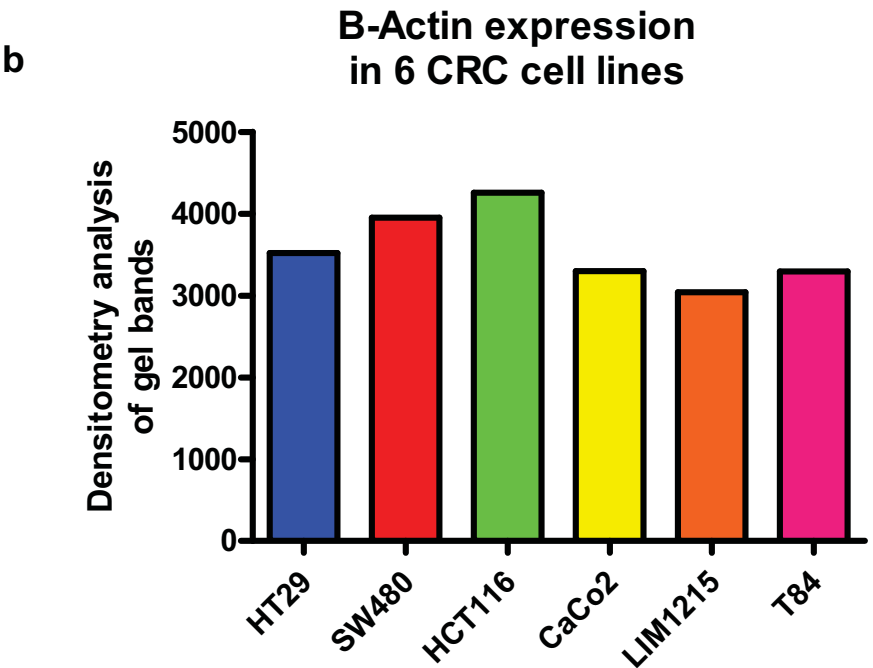
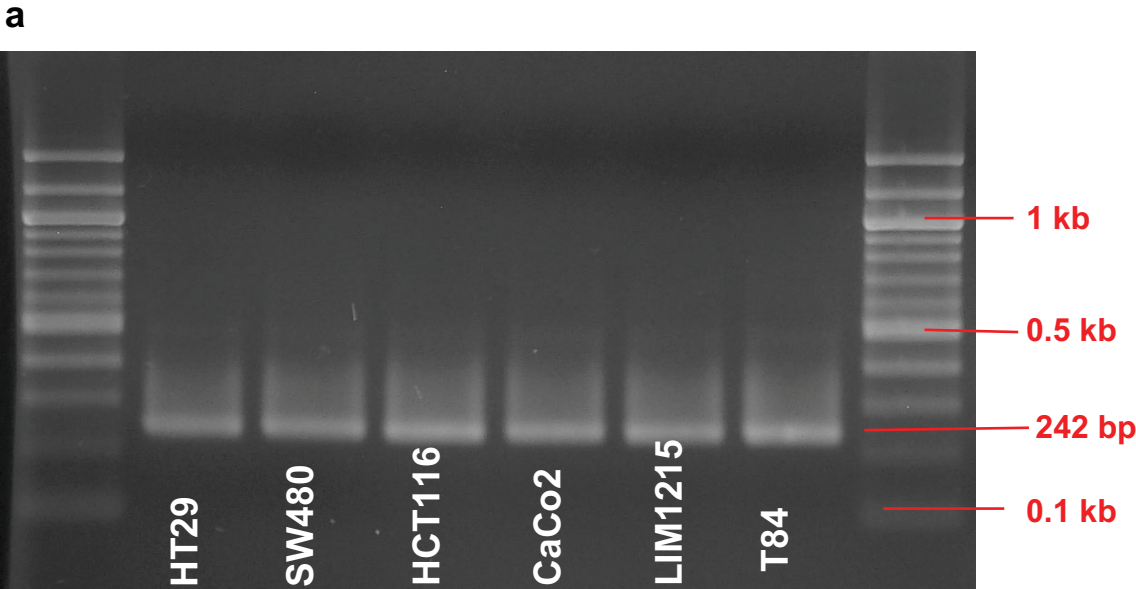


**Figure 4.5: Gel electrophoresis of GPCR43 RT-PCR conducted on extracts from 6 different CRC cell lines and densitometry analysis of the electrophoresis image.**

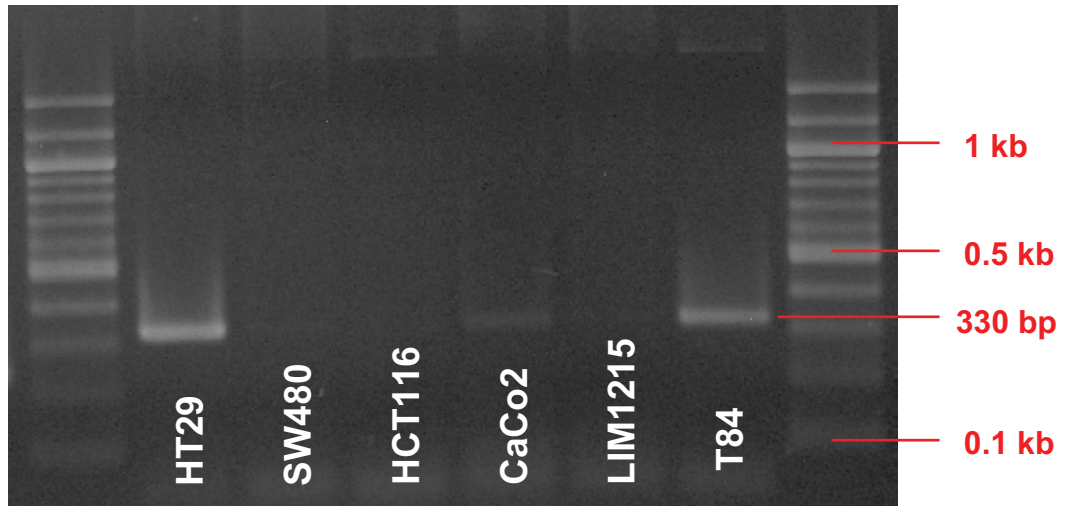
Amplicons from GPCR43 PCR amplifications of either a 330bp length (a) or a 993bp full length (b) from 6 different CRC cell lines.

Results for (a) demonstrate that HT29, CaCo2 and T84 express GPCR43, whereas results for (b) show expression of GPCR43 in HT29 and T84 cells. Densitometry analysis of bands from gel 4.5a is shown in (c) and from gel 4.5b is shown in (d).

The molecular weight markers are shown and the precise details are described in the text.

Figure 4.5

a



b

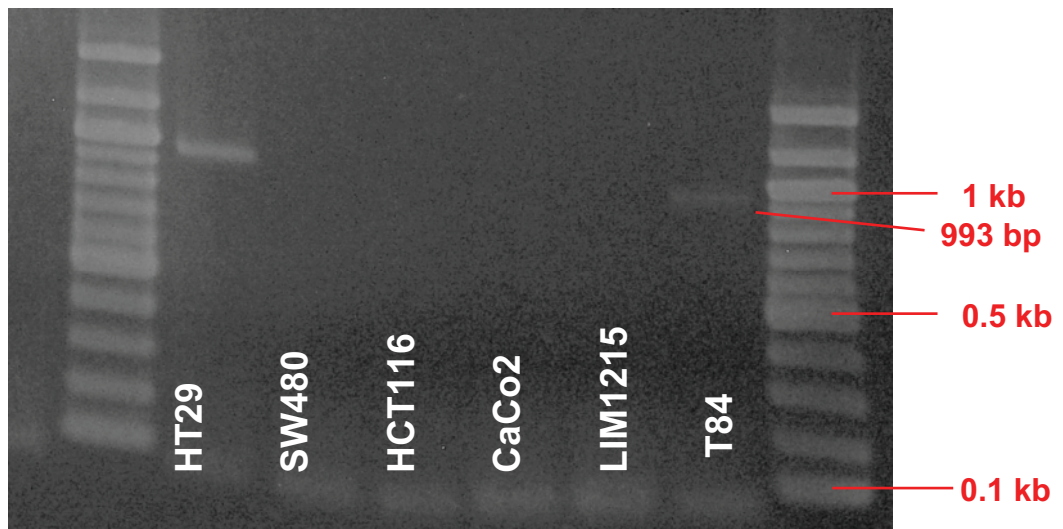
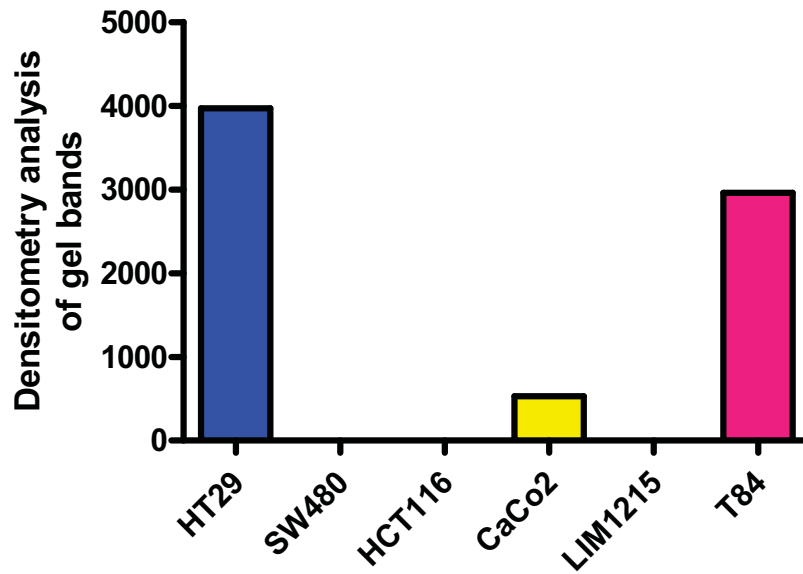


Figure 4.5

**c** GPCR43 expression in 6 CRC cell lines using primers to amplify 330bp



**d** GPCR43 expression in 6 CRC cell lines using primers to amplify 993bp

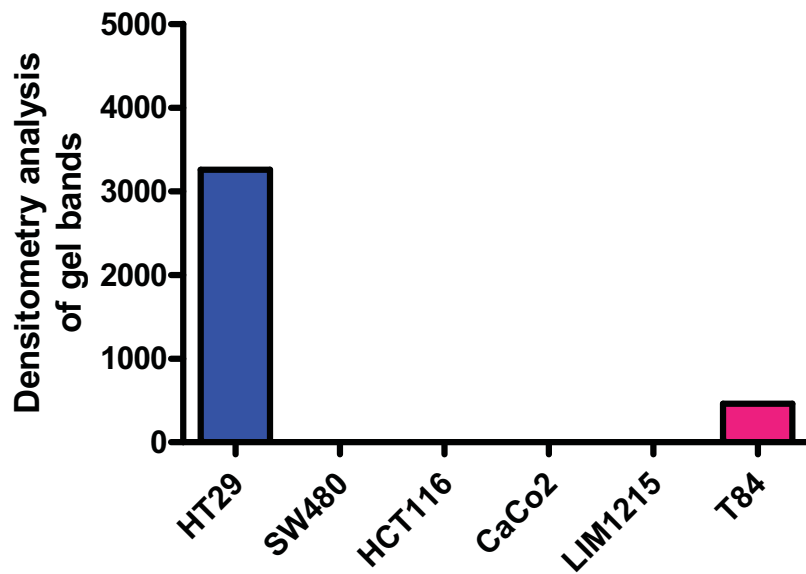
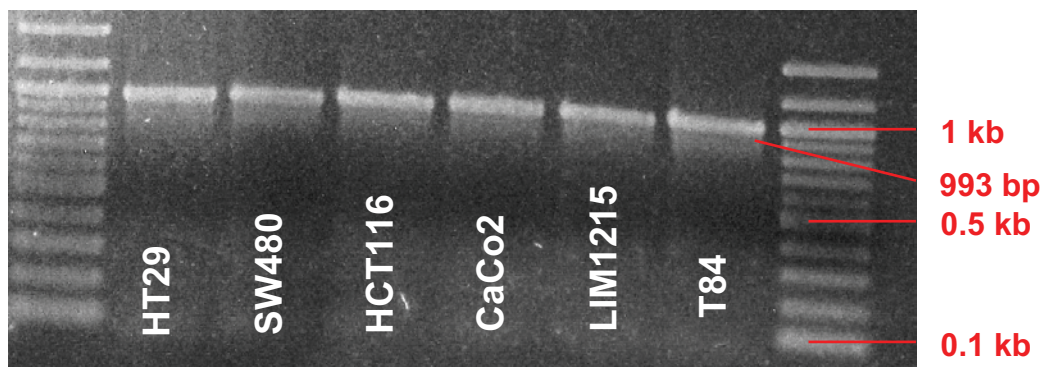




Figure 4.6



**Figure 4.6: Electrophoretic image of RT-PCR of GPCR43 using gDNA extracted from the 6 different CRC cell lines.**

Electrophoretic analysis of PCR amplification products using gDNA extracted from 6 CRC cell lines as the starting template is illustrated. Amplification of the full length sequence of GPCR43 occurred in all samples indicating each of the 6 CRC cell lines possesses the gene encoding GPCR43.

The molecular weight markers are shown and the precise details are described in the text.

**Figure 4.7: Electrophoretic analysis of RT-PCR of the BuA transporter, MCT1, from 6 different CRC cell lines.**

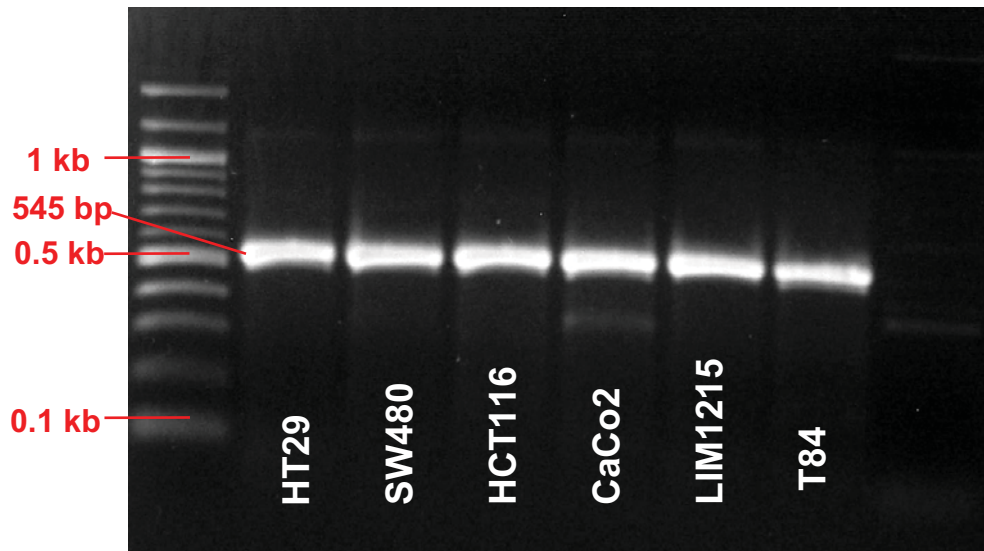
Shown in panel (a) is the PCR amplification products from a RT-PCR conducted using MCT1 primers on the same CRC cell line cDNA samples used in Figure 4.5. Strong amplification in every sample indicates the integrity of the cDNA.

Shown in panel (b) is the densitometry of band intensity of MCT1 expression using Scion Image.

The molecular weight markers are shown and the precise details are described in the text.

Figure 4.7

a



b

